The energy dispersive x-ray detector: A quantitative model

David C. Joy

Citation: Review of Scientific Instruments **56**, 1772 (1985); doi: 10.1063/1.1138092
View online: http://dx.doi.org/10.1063/1.1138092
View Table of Contents: http://scitation.aip.org/content/aip/journal/rsi/56/9?ver=pdfcov
Published by the AIP Publishing

The energy dispersive x-ray detector: A quantitative model

David C. Joy

AT&T Bell Laboratories, 600 Mountain Avenue, Murray Hill, New Jersey 07974

(Received 8 April 1985; accepted for publication 5 June 1985)

When a Si(Li) solid-state energy dispersive detector is used to collect x-ray photons with energies below 2 keV the characteristic peaks in the spectrum show significant deviations from the ideal Gaussian shape observed for higher energy photons. This effect is due to incomplete collection of the charge deposited by the incident photon in the diode. The magnitude of this effect, and the resultant distortion of the spectrum, can be computed by means of a Monte Carlo simulation which models the detector in terms of the three parameters which characterize it, junction depth, diffusion length, and surface recombination velocity. For values of these parameters typical of commercial detectors it is found that the incomplete charge correction can be as high as 30% for a line such as N K_α at 400 eV. By matching simulated and experimental spectral shapes, quantitative corrections for each x-ray line of interest can be computed. The results suggest that alternative design strategies for detectors might permit a higher quality of performance to be achieved at low energies.

INTRODUCTION

Since its initial description in 1966[1] the Si(Li) solid-state energy dispersive x-ray detector has become the most widely applied tool for chemical microanalysis. Despite this popularity, little attention has been paid to the properties of the detector itself. In the context of electron beam x-ray microanalysis any discussion has usually been confirmed to estimating the magnitude of the absorption of soft x rays in the beryllium protecting window, and to the effect of the transmission of high-energy photons through the detector crystal.[2] This is reasonable so long as attention is confined to x-ray photons with energies of a few kiloelectron volts, since in this regime the detector appears to act as a 100% efficient transducer converting a flux of monoenergetic photons into a train of charge pulses having a Gaussian intensity distribution of predictable width about a mean value linearly related to the x-ray energy. Although deviations from the ideal peak shape have been recognized, these are of secondary importance.

With the advent of thin window, or windowless, detectors this situation is changed because it is observed that the peaks generated by low-energy (less than 2 keV) photons tend not to be Gaussian, but display a low-energy "tail" whose relative size and shape may vary dramatically with energy. At the same time the calibration is often found to become nonlinear. Both effects indicate that the detector is no longer completely efficient at converting the photon energy to a measurable charge pulse, and thus these effects are labeled as "incomplete charge" phenomena. While neither effect prevents qualitative microanalysis, the peak shape distortion makes it difficult to measure the integrated intensity under the peak, and the distortion and nonlinearity make the standard procedures for peak overlap correction impossible to apply, so consequently quantitative microanalysis becomes difficult and inaccurate.

Because of the importance of light element microanalysis it would clearly be desirable to be able to overcome these problems, either by improvements in the detector, or by quantifying the effects of incomplete charge collection so that the appropriate corrections could be applied to experimental data. In this paper the characteristics of a solid-state detector are analyzed by means of a simple physical model and a Monte Carlo simulation, and it is shown that the observed spectral distortion effects can be predicted given the semiconductor parameters which describe the detector. By using the model to match experimental spectra from a detector the required correction can be obtained. It is also suggested that an analysis of this type may aid in the development of improved detectors.

I. MODELING THE DETECTOR

Figure 1 shows schematically the typical *p-i-n* diode configuration of a solid-state silicon x-ray detector.[3–5] The detector is divided into three regions. The first region, doped n or n^+, is provided to facilitate the production of an ohmic back contact to the diode. The second region, comprised of intrinsic silicon (usually compensated with lithium) is the "active" region where, when the diode is reverse biased, the material is space-charge depleted. The *p-i-n* geometry allows the active region to be extended to a sufficient depth, typically several millimeters, to capture all the charge produced by photons with energies up to 10 keV or more. The combination of the high resistivity of the intrinsic material and the large bias typically applied also ensures that the depletion region extends through the entire active depth. Therefore, any charge carriers generated in this region will be separated by the depletion field and swept out to the external circuit. The use of intrinsic material also minimizes the capacitance, which is important because if n electron-hole pairs are col-

 0034-6748/85/091772-08$01.30

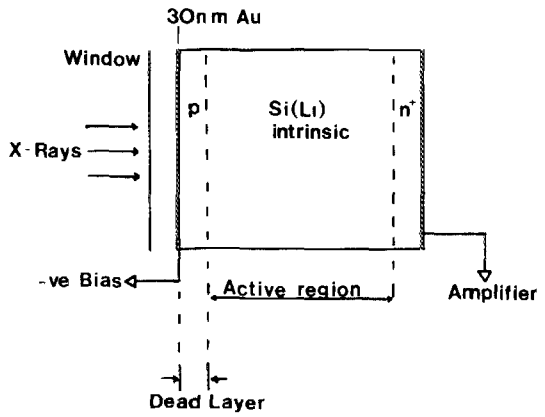

FIG. 1. Schematic drawing of a *p-i-n* diode, solid-state energy dispersive x-ray detector.

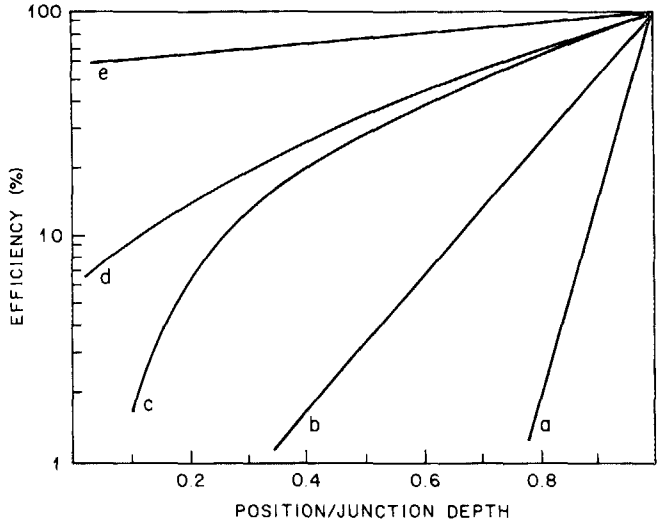

FIG. 2. Variation of charge collection efficiency with source position for a junction at depth 0.2 μ, with (a) $DL = 0.01\ \mu$, $s = 100$, (b) $DL = 0.03\ \mu$, $s = 1$, (c) $DL = 0.1\ \mu$, $s = 100$, (d) $DL = 0.1\ \mu$, $s = 1$, (e) $DL = 0.5\ \mu$, $s = 1$.

lected by the field, then a voltage pulse

$$\Delta V = (ne)/C \tag{1}$$

will be sensed by the input field effect transistor of the preamplifier, where e is the electron charge and C is the effective capacitance of the diode.

The third region is that between the junction (at a depth DD) and the surface. Because of the doping used to form the junction the resistivity of this material will be low, and consequently the space-charge region will not extend significantly into this volume. In the simplest approximation this neutral region, is assumed to possess a finite minority carrier diffusion length DL, so that charge carriers generated at a depth z from the entrance surface would have a probability

$$n = \exp\,[\,-(DD - z)/DL\,] \tag{2}$$

of diffusing to the junction and being collected by the depletion field there. For all except the trivial limiting case where DL is infinite, any charge carriers deposited in this p region will therefore contribute to the incomplete charge.

In practice the entrance surface exerts a strong effect on charge collection efficiency in this region. Trapped charge in the spongy oxide beneath the entrance metallization, as well as electrically active defects introduced by processing, can result in the recombination of some of the charge carrier pairs. Since carriers which recombine do not contribute to the collected charge, the surface thus influences the incomplete charge magnitude. The competition between diffusion towards the recombinant surface and drift towards the junction defines a characteristic depth within which the efficiency of charge collection is effectively zero,[6,7] that is, the presence of the surface produces a "dead layer." This idea can be quantified by rewriting Eq. (2) to allow for the effects of surface recombination. If the surface has an effective normalized recombination velocity of s, then the effective minority carrier diffusion length DE for a carrier produced at depth z below the surface is[8]

$$DE = DL\sqrt{\{1 - [s/(s+1)]\exp(-z/DL)\}}\,. \tag{3}$$

For a perfect, nonrecombining surface, s is zero and thus DE will be constant and equal to DL. For any other surface s is greater than zero and so DE will be less than DL and a function of z. The fractional charge collection efficiency is then, from Eq. (2),

$$n = \exp\,[\,-(DD - z)/DE\,]\,. \tag{4}$$

As s and DL are varied the collection efficiency predicted by Eqs. (3) and (4) changes greatly. Figure 2 plots, as a function of (z/DD), some efficiency profiles for a selection of values of s and DL. At one extreme, for a good surface (s small) and quality material such that $DL \gg DD$, the collection efficiency is close to 100% everywhere (curve e), while the $DL < DD$ and a lossy surface (s large) only charge generated close to the junction is collected with any efficiency (curve a). Intermediate values of s and DL produce a variety of profiles. As shown later values of these two parameters, as well as of DD, can be derived from measurements made on a detector, so a model of the charge collection efficiency, on this set of assumptions, can be generated and used as the basis for subsequent computations.

II. MONTE CARLO SIMULATION

A single parameter description of a *p-i-n* diode, such as its quantum efficiency when used as a detector, can be found by straightforward analytical methods.[9] In this paper a more detailed analysis involving the use of Monte Carlo methods is applied so as to allow the pulse-height distribution of the detector to be characterized. Three steps are involved. First, the depth distribution of the photoelectrons produced by the x-ray photons must be determined, then a subsequent motion of the photoelectrons must be tracked. Finally, the charge collected by the diode as a result of these operations must be calculated.

An x-ray photon gives up all of its energy to a photoelectron in a single collision. The depth distribution of such events can readily be determined, since the absorption of x-rays is described by Beer's law in the form

$$I(z)/I(0) = \exp\,(-z/\lambda)\,, \tag{5}$$

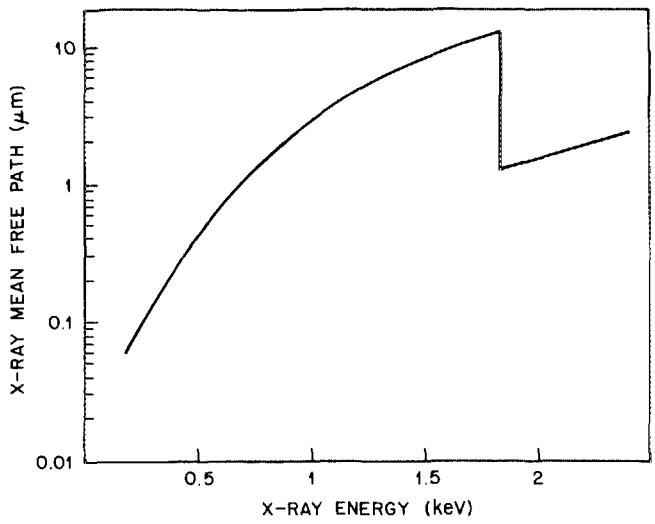

FIG. 3. Mean free path (in microns) as a function of energy for x-ray photons in silicon.

where λ is a mean free path given (in cm) as

$$\lambda = 1/(\rho MA)\,, \tag{6}$$

where MA is the mass absorption coefficient (cm^2/g) for the photon energy of interest in the detector, and ρ is the density (g/cc). Figure 3 plots λ as a function of photon energy for silicon, showing that the value of λ varies from less than 0.25 μ at C K_α, to nearly 14 μ just before the silicon absorption edge. In the simulation the photon is assumed to generate its photoelectron at a depth z from the entrance surface given, from an inversion of Eq. (5), by

$$z = -\lambda \log(\mathrm{RND})\,, \tag{7}$$

where RND is an equidistributed random number lying between 0 and 1. The photoelectron is allowed to leave the generation point in a random direction, and with an energy equal to that of the photon. The range of the electron is calculated using the Bethe energy loss relation,[10] even though for low-energy electrons this formulation is probably not the most accurate available. But as shown in Fig. 4 the range of the electron in all cases is much less than the x-ray photon mean free path, and consequently errors in the calculated electron range are unlikely to be a major source of error. However, although the electron range is small it cannot be neglected, especially as it has been suggested[5,11] that the emission of "hot" electrons from the detector might be responsible for some of the observed effects of incomplete charge collection.

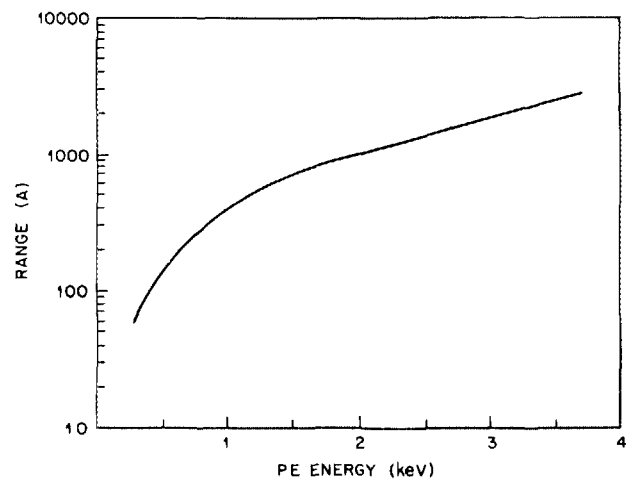

FIG. 4. Calculated photoelectron range in silicon as a function of energy.

The motion of the photoelectron is modeled using a plural scattering Monte Carlo technique.[10] The range is divided into 20 steps of equal length, and the electron energy $E(k)$ at the end of the k th step is calculated from the Bethe relation. The energy deposited during this step is $[E(k-1) - E(k)]$, and if the energy required to create an electron-hole pair is e_{eh}, then the number of charge carriers N created[12] in this portion of the trajectory is

$$N = [E(k-1) - E(k)]/e_{eh}\,. \tag{8}$$

The fraction n of these carriers that are captured and separated by the depletion field depends on the position z of the midpoint of the step.[13,14] If z is equal to, or greater than, DD, then $n = 1$ and all the carriers contribute to the charge pulse. If z is less than DD, n is evaluated using Eqs. (3) and (4). This procedure is repeated for each of the 20 steps of the trajectory, or until the photoelectron leaves the detector. Because the drift velocity of the photoelectron is of the order of 10 m/s, the time for the great majority of the charge to be collected is only a few hundred nanoseconds.[6] Consequently, it is the summed charge evaluated as discussed above that is sampled by the analog-to-digital converter in the pulse-height analyzer and converted to a channel number for presentation in the display. In this simulation the "height" of each pulse is recorded by the computer, in units equivalent to a channel resolution of 15 eV. The graphics display can then be used to emulate that of a conventional multichannel analyzer, adding one count to the appropriate channel at the end of each completed trajectory. In order to make the display closer in form to experimental spectra, an optional Gaussian convolution is provided to allow for the effect of finite energy resolution in the detector. In the data shown here a spread equivalent to a "resolution" of 160 eV FWHM at Mn K_α was used.

For the purposes of this analysis the incomplete charge was defined as that fraction lying outside of (i.e., more than 15 eV away from) the expected channel for the incoming photon energy. This is probably a more restrictive criterion than could be applied in practice, and is also open to the criticism that it represents a smaller percentage shift at high photon energies than at lower energies, but it has the merit of being a simple and consistent definition. In addition to a tabulation of this quantity other parameters such as the apparent calibration error (percentage shift between the computed and expected peak positions) and emitted photoelectron yield were stored. Two versions of the complete program were used. One was written in compiled BASIC and was run on an APPLE II + equipped with a TITAN accelerator board, while the other was written in FORTRAN and was run on a DEC 11-23. Typically, 5000 photons were simulated for each data point or spectrum shown here.

III. RESULTS AND DISCUSSION

It follows from the physical description given above that the magnitude of the incomplete charge depends mostly on the ratio of junction depth DD to the photon mean free path λ. For example, assuming a junction depth of 0.2 μ, typical of values often quoted, and using values of λ taken from Fig. 2, the simulation shows that the incomplete charge varies from only 3% at the Ca K line ($DD/\lambda = 0.025$) to around 30% at the N K line ($DD/\lambda = 0.8$), indicating both the severity of the incomplete charge effect for light elements and its rapid variation with photon energy. An estimate of the magnitude of the incomplete charge can be found by taking the photoelectron range to be zero. The charge produced by any photon traveling beyond the junction would then be collected with 100% efficiency, while the charge generated from any photon not reaching the junction would contribute to the incomplete charge tail. In this approximation,[5,6] the incomplete charge would then be equal to $[1 - \exp(-DD/\lambda)]$.

Including the effects of finite photoelectron range and charge diffusion will modify this result, particularly in two limiting cases. If the material in the entrance region has a diffusion length which is large compared to the junction depth, and if the surface recombination velocity is small, then the efficiency with which the charge is collected from this region could be so high that much of the "incomplete charge" might actually appear as part of the "complete" charge signal. The other limiting case would be when the region between the surface and the junction had a diffusion length which was very much less than the junction depth. In that case photons not reaching the junction would produce no charge contribution, except for any small fraction resulting from photoelectrons traveling across the junction. Thus, for a true "dead layer" beneath the entrance surface there would be no visible incomplete charge effect, instead, the efficiency of the detector would be lowered by an amount equal to the fraction of photons failing to reach the junction.

Figure 5 compares values of incomplete charge collection computed from the Monte Carlo simulation, and plotted as a function of DD/λ for a variety of values of DL, DD, and s, with the expression $[1 - \exp(-DD/\lambda)]$. It can be seen that the computed values generally lie close to the analytical line, although in some cases the error is as high as an order of magnitude when the detector parameters fall into one of the two limiting categories discussed above. The analytical expression therefore sets only an upper limit to the magnitude of the incomplete charge, and it is necessary to find values for s, DD, and DL for the detector of interest and run the simulation for each x-ray line to be used when an accurate quantitative correction is required.

The energy distribution of the incomplete charge also varies as a function of the diffusion length and surface recombination parameters, as illustrated in Fig. 6 which shows spectra for the Ca K line, and an arbitrarily chosen junction depth of 1 μ. When the diffusion length is small and the surface recombination is high ($s = 100$) the incomplete charge is concentrated at the bottom end of the spectrum, producing a low-energy peak similar in appearance to that often observed in spectra from ultrathin window detectors[15] and usually attributed to preamplifier noise. Between this low-energy peak and the real calcium peak the spectrum is flat, so that in the corresponding experimental situation to this the incomplete charge would probably be missed since the flat region would be hidden by bremsstrahlung, and the low-energy peak would be eliminated by the discriminator. The real form and magnitude of the incomplete charge would probably only be visible in spectra excited by x-ray fluorescence.[2,7] As the diffusion length is increased the low-energy peak is redistributed over the spectrum, eventually taking up the familiar form of a broadening, or tail, on the low-energy side of the characteristic peak. Therefore, depending on the relative values of the parameters describing the detector, the incomplete charge can appear in a large variety of ways, many of which may make it hard to observe experimentally. Provided the mean free path λ for the inci-

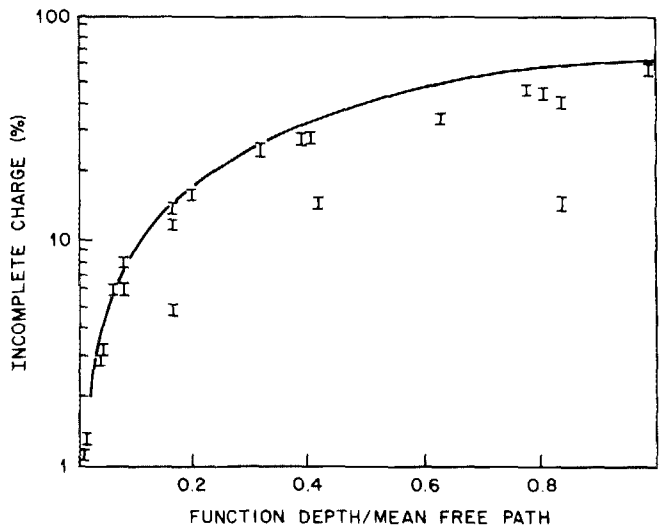

FIG. 5. Computed value of incomplete charge collection for a silicon detector plotted as a function of the junction depth divided by the x-ray mean free path. The dotted line is the theoretical estimate given by Shima *et al.* (1983).

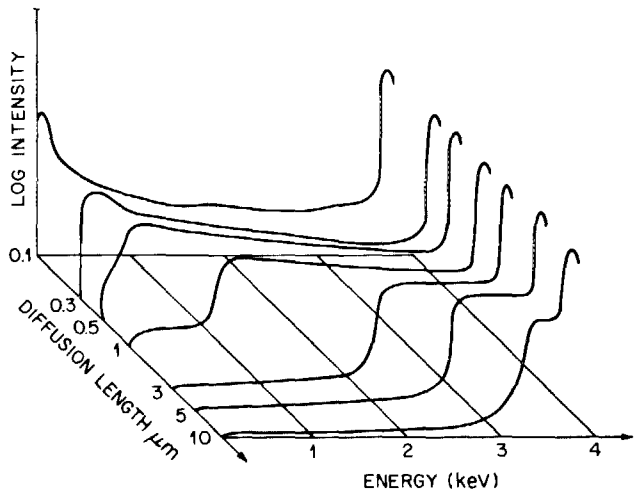

FIG. 6. Computed spectra for Ca K line excitation of a detector, with a junction of 1 μ and a value of $s = 1$, plotted as a function of the recorded energy and diffusion length. For clarity the relative intensity scale is logarithmic. The data was calculated assuming a detector resolution of 160 eV FWHM at Mn K.

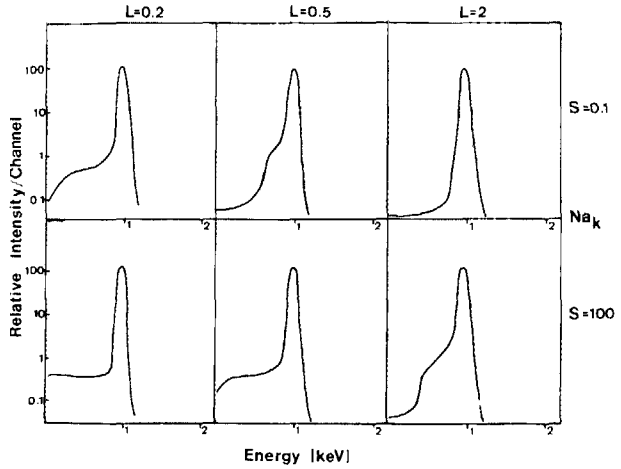

FIG. 7. Computed peaks shapes for Na K line with detector diffusion lengths (L) of 0.2, 0.5, and 2 μ and normalized surface recombination rates (s) of 0.1 and 100, for a junction depth of 0.2 μ.

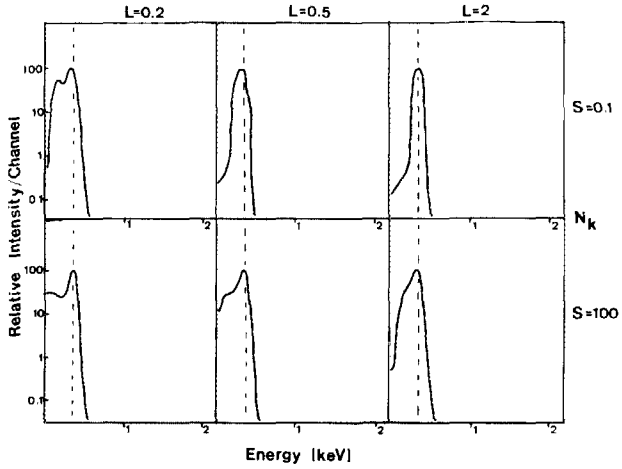

FIG. 9. As in Fig. 7, data for N K line.

dent photon is greater than the junction depth DD, this form of behavior will always be observed.

This is illustrated in more detail in Figs. 7, 8, and 9 which show spectra computed for Na, O, and N for a junction depth of 0.2 μ, assuming three values of diffusion length (0.2, 0.5, and 2, μ) and two different rates of surface recombination. For Na (Fig. 7), the effect of changing these parameters is to change the incomplete charge from a flat step ahead of the peak ($DL = 0.2, s = 100$) to a low-energy broadening of the peak when the diffusion length is raised and the surface recombination is reduced. For the equivalent set of conditions, the appearance of the oxygen peak (Fig. 8) is substantially different, because the photon mean free path is smaller and so the incomplete charge is much higher. Low values of the diffusion length lead to a severely distorted peak, and in all cases threre would be visible deviations from the expected Gaussian shape. This is more evident in the data for nitrogen (Fig. 9) where, for all but the most favorable set of parameters ($DL = 2$, $s = 0.1$), the peak is heavily distorted. However, for each of these lines there is a clear distinction between the characteristic peak and the incomplete charge. But if similar calculations are made for the carbon line (Fig. 10) the situation looks considerably different. As can be seen from the line indicating the expected position for carbon, the peak in the spectral intensity now falls below the predicted energy, corresponding to an apparent shift in calibration. Further, for several sets of conditions the peak is now nearly gaussian in shape again even though a higher energy edge (nitrogen) under the same conditions would show significant distortion.

This anomalous behavior, which is confirmed experimentally, results from the fact that the photon mean free path (0.13 μ) is now smaller than the junction depth.[16,17] A majority of the photons, therefore, do not reach the junction, and the characteristic peak disappears. The peak observed is actually the incomplete charge, although in the absence of the proper characteristic peak the original definition is no longer applicable. Although the peak may appear to be of good shape, disguises the fact that a measurement of this intensity would not necessarily provide any information about the magnitude of the carbon signal which produced it. A measurement of the junction depth DD would be desirable

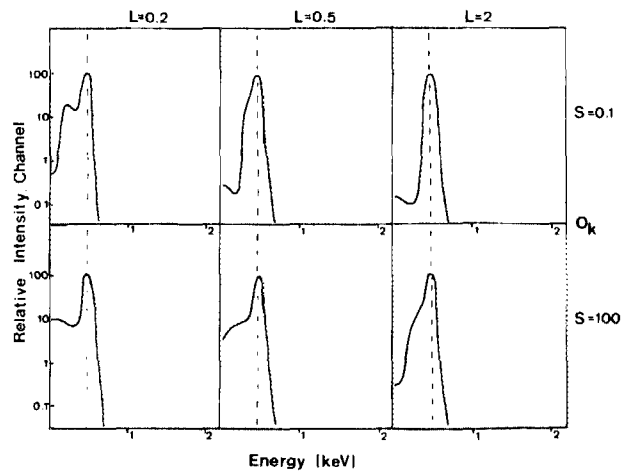

FIG. 8. As in Fig. 7, data for O K line.

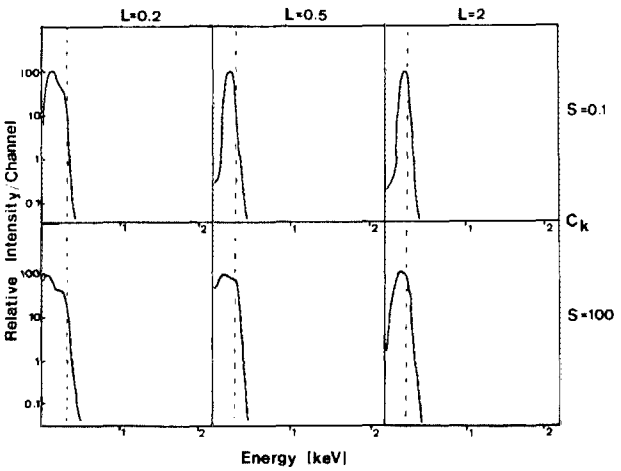

FIG. 10. As in Fig. 7, data for C K line.

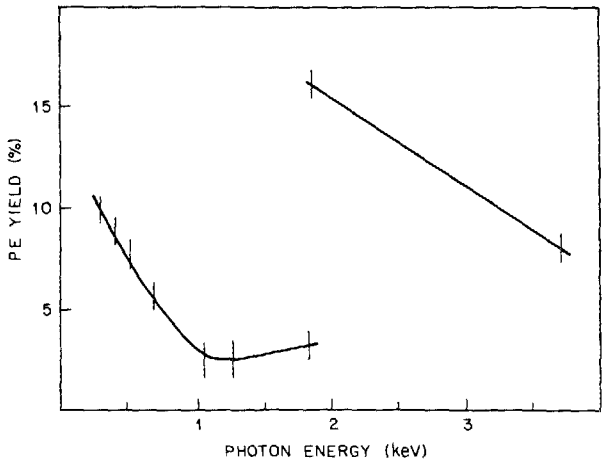

FIG. 11. Computed yield (emitted electrons per incident photon) of hot electrons from entrance face of a silicon detector, plotted as a function of incident photon energy.

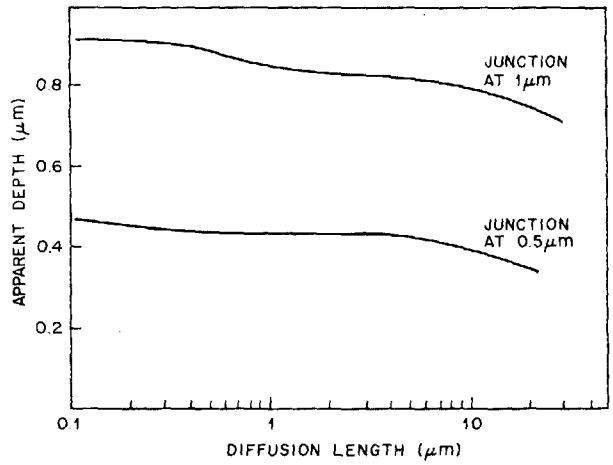

FIG. 12. Variation of apparent "dead layer" thickness, calculated from the jump ratio at the silicon absorption edge, with diffusion length. Data simulated for junction depths of 0.5 and 1 μ, assuming $s = 1$.

on any system from which quantitative results are required, so that misleading data is not produced from peaks with mean free paths falling below this value. The observation of an apparent shift in calibration can also be used to indicate the onset of this problem. It should be noted that the calibration shift will, in general, vary when the bias is changed, because this will slightly modify the position of the onset of the depletion layer relative to the incident surface, and hence the applicable value of *DD*.

Finally, it has been suggested[5] that the emission of hot electrons from the entrance face of the detector might be responsible for some of the incomplete charge. Figure 11 shows the computed magnitude of this emission for the lines from carbon to calcium. The data show a systematic variation, similar to that for the photon mean free path, with an average value of about 1 photoelectron emitted per 100 incident photons (1%), although for the worst case (just below the silicon absorption edge) the figure rises to nearly 16%. Although this is a high figure it must be remembered that before being emitted the photoelectron will have deposited some, or probably most, of its energy and consequently the "loss" in charge will be much lower than this figure. In the low-energy part of the spectrum where incomplete charge is most serious the effect of electron emission is clearly not a major factor.

IV. ESTIMATING DETECTOR PARAMETERS

To apply this simulation to calculate the magnitude and distribution of incomplete charge it is necessary to know the relevant parameters for the detector of interest. Conventionally, the dead layer has been measured by recording the jump in recorded spectral intensity which occurs at the Si *K* absorption edge (1.83 keV), and assuming that the observed jump ratio is proportional to the product of the difference of the mass absorption coefficients on either side of the edge and the dead layer thickness.[17] An application of the simulation, for energies on either side of the absorption edge, shows that such a measurement does, in fact, give a value which correlates well with the junction depth. Figure 12 plots the "dead layer" thickness that would be calculated from this assumption for two different values of junction depth. For realistic values of the diffusion length, in the range of 1 μ or so, the "measured" value would be within 20% to 30% of the correct value, although the answer is always an underestimate. For high values of diffusion length the error could be much larger (i.e., 60% at $DL = 50\ \mu$ for $DD = 0.2\ \mu$), but such a value is unlikely to be met in practice.

While this method can provide a good value for *DD*, it cannot provide any values for *DL* and *s*. However, given the junction depth a series of simulations of the type shown in Fig. 6 can then be made for a range of values of *DL* and *s*. A comparison of such plots with experimental spectra, especially those obtained by x-ray fluorescence which contain no electron induced bremsstrahlung, allows a match to be found. Since the form of these spectra shows a characteristic variation with *DL* and *s*, obtaining approximate numerical values is straightforward. These values can then be further refined by detailed comparisons between observed and computed peak shapes, such as those illustrated in Figs. 7–9.

An alternative approach has been suggested[3] in which the silicon detector crystal is observed in the charge collection [electron beam induced current (EBIC)] mode of the scanning electron microscope. The detector is irradiated at energy E by an electron current I_b, and the short circuit current I_{cc} generated by the detector is measured to give the gain G, where

$$G = I_{cc}/I_b \ . \tag{9}$$

The gain is then plotted as a function of E. An extrapolation of the linear portion of this plot to zero gain then gives an energy value E_c. The electron range is silicon at the energy E_c determined, for example, for Fig. (4), is then equated to the junction depth. This situation is also readily simulated by a Monte Carlo model, and Fig. 13 shows computed values of G, as a function of E, for some values of *DL* and *s* at a junction depth of 1 μ. Extrapolating the linear region gives an intercept at just below 5 keV, corresponding to a range of

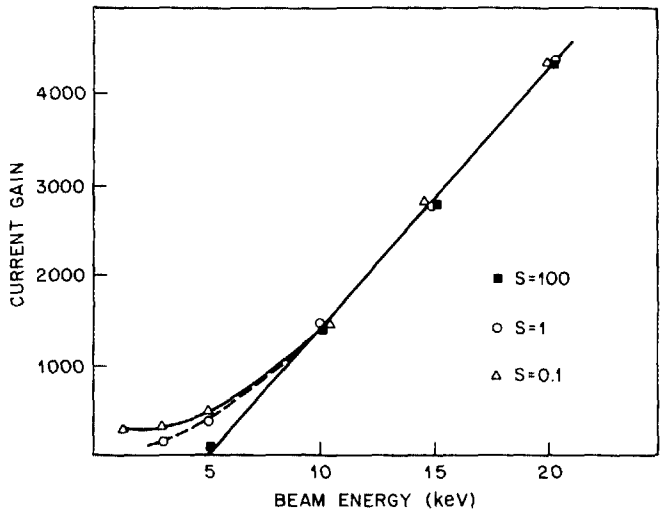

FIG. 13. Computed variation of EBIC charge collection current gain with incident electron beam energy for a silicon detector with its junction at a depth of 1 μ, and a diffusion length of 1 μ.

0.95 μ. The estimate obtained in this way is an excellent measurement of the junction depth and has the advantage of being applicable even to very shallow junctions. In addition the shape and extent of the deviation from linearity depends sensitively on the values of *DL* and *s*, so experimental and computed results can readily be matched to find these parameters. The obvious drawback of this method is that it cannot be applied to a working detector, and so is only of use during the manufacturing process.

V. CONCLUSIONS

The simulation discussed here provides a quantitative model of the behavior of an energy dispersive x-ray detector. When appropriate values of the detector parameters are supplied, this procedure permits the response of the system to photons of different energy to be computed in sufficient detail to allow the magnitude of incomplete charge collection, and the ensuing peak distortion, to be determined. These results indicate that with parameters typical of those found on current commercial detectors (e.g., $DD = 0.2$ μ, *DL* about 1 μ, and *s* of the order of unity), the incomplete charge effect is considerable (in excess of 10%) for all peaks below Na *K*, even though the visual evidence of this is masked by the way in which this charge is distributed across the spectrum. When performing quantitative chemical microanalysis the data derived from a simulation of this type can then be used to make corrections to the peak integrals to account for the incomplete charge collection.

Although the agreement between experimentally observed spectra and those simulated here is good, further refinements of the program are desirable. In particular, interactions between the detector and its associated electronics[18] might be an additional source of spectral distortions, and so should be considered. Other contributions to incomplete charge have also been proposed, including the photoelectric capture of a low-energy x-ray by the Si *K* or *L* shell, resulting in an ionization relaxed by Auger emission,[19] and the addition of such a mechanism to the existing model would be straightforward. Finally, it is also possible that a simulation such as this could be used to investigate some of the other properties of the detector, in particular, their energy resolution. The resolution experimentally observed (typically 2.5% FWHM at 6 keV) is much better than would be predicted from simple statistical arguments based on the number of charge carriers produced. A detailed analysis might indicate how the Fano factor, which determines the resolution, is affected by the semiconductor properties of the detector.[20,21]

In the absence of direct evidence to the contrary it seems likely that the design of current energy dispersive x-ray detectors is mostly the result of an empirical development procedure from particle detectors. While this process has been led to x-ray detectors with more than adequate performance in the midenergy range (3–10 keV), it is obvious from the data presented here that the semiconductor parameters which represent the detector are not necessarily optimized for other energy ranges. Several options appear to be available to improve the performance of x-ray detectors. One route would be to attempt to "kill" the region between the surface and the junction so as to raise the recombination velocity *s* and lower the diffusion length *DL*. At the limit when DL is zero the incomplete charge effect, as demonstrated above, will disappear but the efficiency of the detector will fall rapidly with energy. The opposite, and more efficient, approach would be to improve the technology of the junction by such techniques as a programmed ion implant, followed by a laser anneal, to give the highest possible value of *DL* while maintaining a low rate of surface recombination. As shown in the simulations this would significantly improve peak shapes without sacrificing efficiency.

Finally, it might be productive to abandon the concept of using a single detector to cover the whole x-ray spectrum of interest, and to consider instead splitting the spectrum into two or three ranges and then optimizing a detector design for each. While the conventional design is perfectly acceptable for energies between 2 and 15 keV, and higher energies can efficiently be handled by a germanium detector, the best low-energy detector is seen to be either a very shallow junction, or a surface barrier device, since with the junction essentially at the surface the incomplete charge magnitude is drastically reduced, and the effect of the surface states is minimized. Because only low-energy photons would need to be detected the depletion region required is shallow, and on high quality intrinsic material sufficient depletion depth would, in fact, be generated, even in the absence of an applied reverse bias. Thus, a specialized low-energy detector could offer both improved performance and simpler construction.

ACKNOWLEDGMENTS

The author wishes to thank G. Aden, G. Cliff, J. Colby, C. E. Fiori, W. Hardy, D. E. Newbury, A. Sandborg, J. M. Titchmarsh, and R. Trammel for helpful discussions related to various aspects of this paper.

[1]E. Elad and M. Nakamura, Nucl. Instrum. Methods **41**, 161 (1966).
[2]K. M. Barfoot, I. V. Mitchell, L. Avaldi, and H. L. Eschbach, Nucl. Instrum. Methods **B5**, 534 (1984).
[3]L. G. Wolfgang, J. M. Abraham, and C. N. Inskeep, IEEE Trans. Nucl. Sci. **NS-13**, 30 (1966).
[4]J. Muller, IEEE Trans. Electron. Devices **ED-25**, 247 (1978).
[5]K. Shima, S. Nagai, T. Mikuma, and S. Yasumi, Nucl. Instrum. Methods **217**, 515 (1983).
[6]J. M. Caywood, C. A. Mead, and J. W. Mayer, Nucl. Instrum. Methods **79**, 329 (1970).
[7]F. S. Goulding, Nucl. Instrum. Methods **142**, 213 (1977).
[8]L. Jastrzebski, J. Lagowski, and H. C. Gatos, Appl. Phys. Lett. **27**, 537 (1975).
[9]H-S. Lee and S. M. Sze, IEEE Trans. Electron. Devices **ED-17**, 342 (1970).
[10]R. L. Myklebust, D. E. Newbury, and H. Yakowitz, NBS Special Pub. No. 460 (1976), p. 105.
[11]J. Llacer, E. E. Haller, and R. C. Cordi, IEEE Trans. Nucl. Sci. **NS-24**, 53 (1977).
[12]B. Akamatsu, J. Henoc, and H. Henoc, J. Appl. Phys. **52**, 7245 (1981).
[13]R. J. Soukup and G. P. Bartunek, J. Appl. Phys. **53**, 4428 (1982).
[14]H. J. Leamy, J. Appl. Phys. **53**, R51 (1982).
[15]G. Cliff, D. M. Maher, and D. C. Joy, J. Microscopy **136**, 219 (1984).
[16]P. J. Statham, NBS Special Pub. No. 604, 1981, p. 127.
[17]R. G. Muskett, NBS Special Pub. No. 604, 1981, p. 97.
[18]R. Benumof and J. Zoutendyk, J. Appl. Phys. **56**, 2964 (1984).
[19]D. E. Newbury (private communication).
[20]R. W. Fink, NBS Special Pub. No. 604, 1981, p. 5.
[21]R. Y. Deshpande, Nucl. Instrum. Methods **75**, 245 (1969).